Liquid Crystals
Publication details, including instructions for authors and subscription information:
http://www.informaworld.com/smpp/title~content=t713926090

The Morphology of Liquid-Crystalline Polymers and the Possible Consequences for their Rheological Behaviour

L. Lawrence Chapoy[a]; Bjørn Marcher[a]; Knud H. Rasmussen[a]
[a] Instituttet for Kemiindustri, The Technical University of Denmark, Lyngby, Denmark

To cite this Article Chapoy, L. Lawrence , Marcher, Bjørn and Rasmussen, Knud H.(1988) 'The Morphology of Liquid-Crystalline Polymers and the Possible Consequences for their Rheological Behaviour', Liquid Crystals, 3: 12, 1611 — 1636
To link to this Article: DOI: 10.1080/02678298808086625
URL: http://dx.doi.org/10.1080/02678298808086625

LIQUID CRYSTALS, 1988, VOL. 3, NO. 12, 1611–1636

The morphology of liquid-crystalline polymers and the possible consequences for their rheological behaviour

by L. LAWRENCE CHAPOY†, BJØRN MARCHER‡ and KNUD H. RASMUSSEN

Instituttet for Kemiindustri, The Technical University of Denmark, DK-2800 Lyngby, Denmark

(Received 29 June 1987; accepted 16 March 1988)

Polymer liquid crystals can occur as polydomain materials where the domain size may be tens of microns. While the material within each domain may be characterized by a common order parameter, the directors of the domains can be more or less randomly distributed. Since the transition from polydomain to monodomain material only involves the removal of grain boundaries and the alignment of directors, the free energy change must necessarily be small. Such a transition can readily be achieved, therefore, by the action of any external field: electrical, magnetic, stress or surface. In this work optical photomicrographs of polymeric liquid crystals with widely varying and in some cases well controlled morphologies are presented. Probable dependence of rheological behaviour on morphology is also discussed. Such dependence is expected to be considerable under certain conditions. Due to experimental and sample limitations, however, direct correlations of rheology and morphology are sparse. Morphological consequences for the rheology of liquid-crystalline materials can be exemplified by the following possibilities. In contrast to the case of isotropic melts, wall effects can be non-negligible. Zero shear rate rheological parameters are not expected to be uniquely defined quantities since the domain sizes are large and the director may not be effectively averaged over typical sample dimensions. Non-zero shear-rate measurements of rheological parameters is effected by the propensity of: (1) individual domain directors to align under the influence of a stress field and (2) flow alignment to dominate surface-induced alignment above some critical shear rate. The effects might be manifested by a non-newtonian regime as well as yield stress behaviour and thixotropy. The kinetics of relaxation from mono- to poly-domain material has implications for the dynamic response and rheological hysterises of the material.

1. Introduction

The introduction of commercial thermoplastic materials designed to be processed in the thermotropic liquid-crystalline state, has stimulated interest in the study of liquid-crystalline polymers in the bulk state. This topic has been the subject of several reviews [1–4]. Heretofore sparse rheological measurements on polymeric liquid crystals have been confined to very thin highly aligned samples with the goal of determining the anisotropic elastic constants and viscosity coefficients as required by, for example, the Leslie–Eriksen formulation [5, 6]. Such samples are monodomain materials characterized by a single director defined by an imposed external field as shown schematically in figure 1-1. For the bulk state, the situation is not so simple in as

† To whom correspondence should be addressed. Present address: Istituto Guido Donegani, Via G. Fauser 4, 28100 Novara, Italy.

‡ Present address: Danaklon A/S, Engdraget 22, 6800 Varde, Denmark.

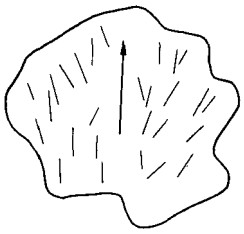

(1)

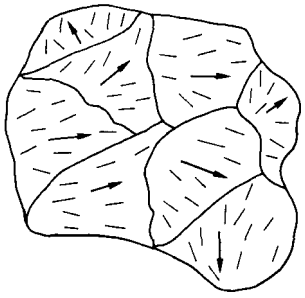

(2)

Figure 1. A schematic diagram depicting (1) a monodomain sample and (2) a polydomain sample. Note that the long range order in each of the domains in (2) is similar to that in (1).

much as the material can exist in a polydomain morphology. The order parameter will be a material constant which will be common to the ensemble of domains, but the director characterizing alignment of the respective domains can be more or less randomly distributed in space, as shown schematically in figure 1-2. The exact nature of the domain boundary as a true grain boundary or optical artifact as in band textures is currently a topic of discussion [4, 7].

Since the domain size can be of the order of a few tens of microns, there will be about 10^{12} domains/litre giving a concentration of 10^{-11} molar. A polymer of molecular weight 10^5 would have about 10^{21} molecules/litre in the bulk or a concentration of 10^{-2} molar, i.e. 10^9 greater than the concentration of domains. Since the transformation from polydomain to monodomain material only involves the removal of these few grain boundaries or disclinations and the alignment of the directors, the free energy change is extremely small. The molecular order as specified by the order parameter is already present in the polydomain material as it is an intrinsic property of the liquid crystal. The situation is thus exactly analogous to the free energy difference between a dendritic polycrystalline material and a single crystal of the same material with the identical crystal structure. A zero order thermodynamic estimate of the free energy difference would be nil.

The implications of this situation for rheology is that while the viscoelastic parameters must be critically dependent on the given morphology, the morphology itself will not be unambiguous in the quiescent state since it will be strongly dependent on history as well as interaction with sample walls. Since free energy changes are small, coupling with external fields can provide dramatic changes in morphology and

furthermore will provide little driving force for randomization when the external fields are removed, implying slow relaxation to the idealized unperturbed state. This requires the co-operative movement of a large number of molecules to deviate spontaneously from the director defined by the monodomain sample in a swarm-like fashion with the accompanying formation of a domain wall disclination. External fields can encompass viscous flow fields, magnetic and electrical fields as well as interactions with surfaces.

Such observations regarding the apparent lack of reproducibility of viscosity data have been made and have been ascribed to the ambiguous nature of the morphology in the quiescent state and its dependence on rheological history [3, 4, 8, 9] and texture [10]. Similarly, unusually slow relaxations to the quiescent state have been observed [4, 11–13]. The implication of these experimental facts is that rheological measurements alone can be inconclusive and that they should be accompanied by simultaneous birefringence (rheo-optical studies) [3] or small angle light scattering measurements [14].

Regardless of the exact morphology of the quiescent state, it appears that the imposition of a shear field ultimately leads to monodomain sample as shown schematically in figure 1-1 [3, 9]. This transition is accompanied by an apparent yield stress and a precipitous drop in melt viscosity at very low shear rates, region I in the nomenclature of Onogi and Asada [15]. The occurrence of such a yield stress has been observed, though not always [16], for both low molar mass [10, 17] and polymeric [3, 9, 18] liquid crystals. The kinetics for the reformation of structure can be manifested by non-linear effects in the dynamic mechanical responses at a frequency ω, for which $1/\omega \approx \tau$, the time constant of the reformation kinetics [19, 20]. The possibility that wall effects can contribute to the observed yield stress has also been discussed, but the question has not been resolved due to conflicting experimental evidence [10, 16, 20, 21]. Specifically, we can consider the case of homeotropic alignment in the quiescent state for which the director is forced to align itself with the flow field above some critical shear rate, $\dot{\gamma}_c$, giving rise to a non-newtonian regime [22]. Note that this is the hydrodynamic analogue of the Fréedericksz transition. Conflicting experimental evidence regarding the yield stress question is probably due to, at least in part, the ill-defined nature of the quiescent state, and the lack of simultaneous rheological and morphological studies. In this regard sample preparation could be of appreciable significance.

The polydomain structure of liquid-crystalline materials has been the source of comparison with regard to the rheological properties of filled materials and their yield stress behaviour [23–25].

The results presented in this study show that the same material can exist in a wide variety of morphological modifications each of which will will necessarily have its own rheological response. The materials under study are cholesteric, lyotropic solutions of poly-[N^{ε}-(9-Carbazolyl-carbonyl)-L-lysine], PKL, a helical forming polyaminoacid similar to poly-[γ-benzyl-L-glutamate], PBLG, which has been synthesized with the aim of investigating the effect of long range order on the photoconductive and spectroscopic properties [26, 27], especially for well-controlled monodomain morphologies. PKL seems to show an unusual propensity for forming varied morphologies. Many of the features of lyotropic polymers are common to thermotropic polymers albeit in another range of temperature and stress, so it would appear that the basic understanding derived through this work would be applicable to the rheology and melt processing of thermotropic polymers.

2. Results and discussion

(*a*) *The effects of walls*

The fact that walls can propagate surface alignment over macroscopic dimensions, tens of microns, for liquid-crystalline materials has been known at least as far back as the Riwlin measurements in 1923 [13]. While extensive investigations of wall effects have been made for low molar mass liquid crystals [28], the situation for polymeric liquid crystals is not clear.

For cholesteric lyotropic polymers it has been found that the wall planes of the cell play an important part in forming an aligned cholesteric structure with the rod axis of the cholesteric molecules and hence the retardation lines parallel to the walls. For thick cells, the z direction in figure 2, the macroscopic alignment spontaneously propagates 100–200 mm as evidenced by parallel cholesteric retardation lines perpendicular to x propagating from the walls into the bulk of the sample when viewed between crossed polarizers in the z direction, as shown in figure 3 for PKL. In the interior of a sample of sufficient thickness the director randomizes through the formation of domains [4].

As the sample thickness in the z direction decreases, approaching twice the propagation length, cholesteric lines are observed uniformly parallel to the y direction across the entire cell (indicating a cholesteric helical axis parallel to the z direction) when viewed from the x direction, cf. figure 4-2. In addition a few lines are observed perpendicular to the x direction at the edges when viewed from the z direction, cf. figure 4-1, giving a concentric arrangement of cholesteric lines which if a hypothetical observation could be made in the y direction, would be that shown schematically in figure 4-3. Note in this case there is no bulk sample as such and that wall effects are dominant. When viewing the sample in the z direction, no structure is observed in the interior of the sample because this represents a random planar distribution of molecules, i.e. an order parameter, $\langle P_2 \rangle$ of $-1/2$ for the limiting case. Observations corresponding to figures 4-1 and 4-2 are shown in figures 5-1 and 5-2, respectively for PKL. Such effects have been alluded to previously by Robinson [29, 30] for PBLG and Onogi *et al.* [4] for hydroxypropyl cellulose, HPC. Note that the micrographs in figure 5 are truly representative of a monodomain sample and in fact show better alignment than that implied in Robinson's model.

As the thickness in the z direction decreases still further approaching that of the cholesteric line spacing, typically of the order of 20 μm, a spontaneous phase change takes place to that of a homeotropic nematic in which the director is defined by the z axis [31]. Figures 6-1 to 6-3 show the time evolution of the homeotropic phase in

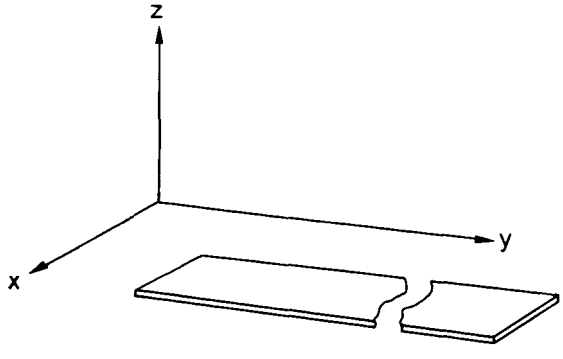

Figure 2. A capillary cell having rectangular cross section.

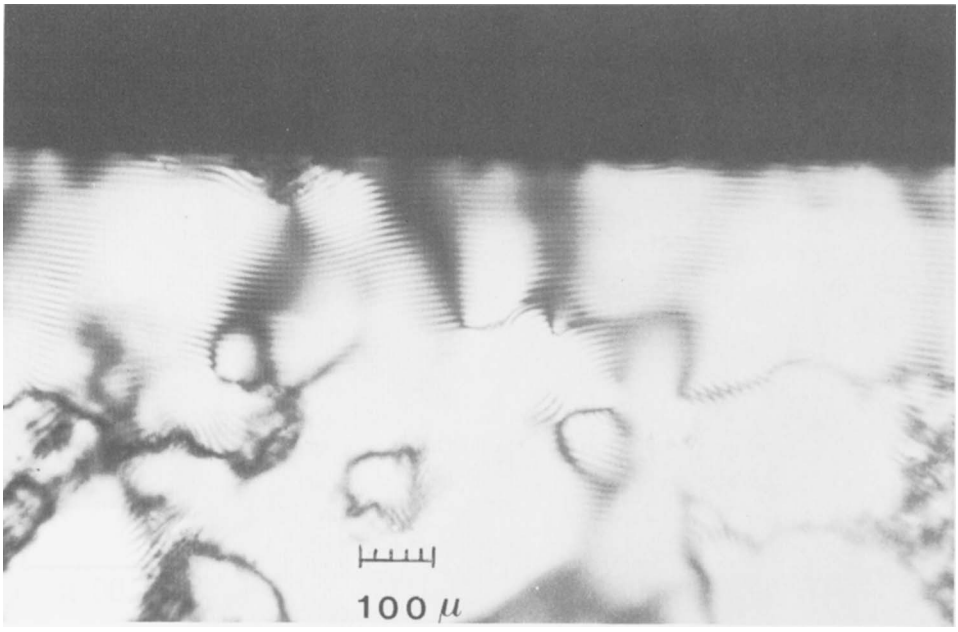

Figure 3. A room temperature polarized photomicrograph of a bulk sample of PKL lyophase in a cuvette 1 mm thick. Note the spontaneous wall orientation. The volume fraction, Φ, of PKL is 0·154 and the solvent is tetrahydrofuran; the PKL used is an unfractionated broad molecular weight sample as described previously [26].

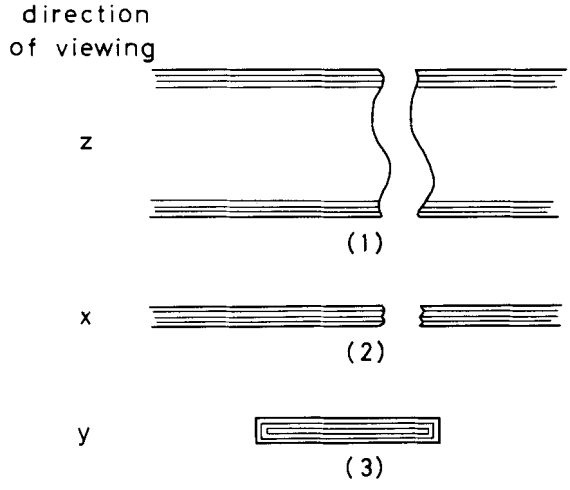

Figure 4. A schematic diagram of a cholesteric phase in the capillary shown by figure 2 for which wall orientation dominates. (1), (2) and (3) show viewing in z, x and y directions, respectively with the idealized cholesteric wall ordering indicated. (1) and (2) can be observed directly. (3) is a composite deduced from the observations of (1) and (2); this is not directly observable.

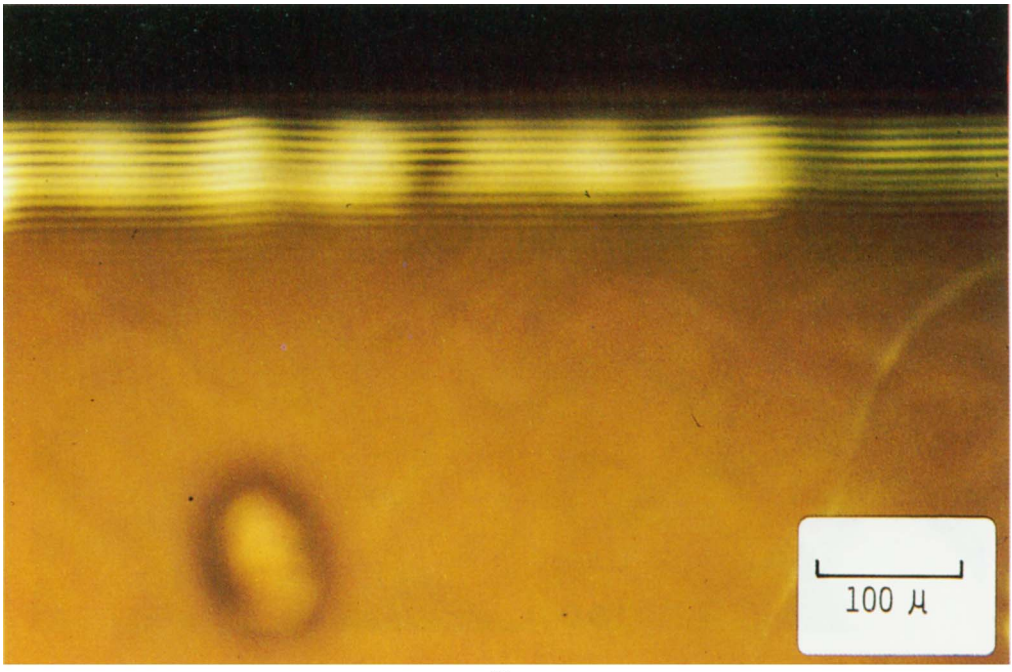

(1)

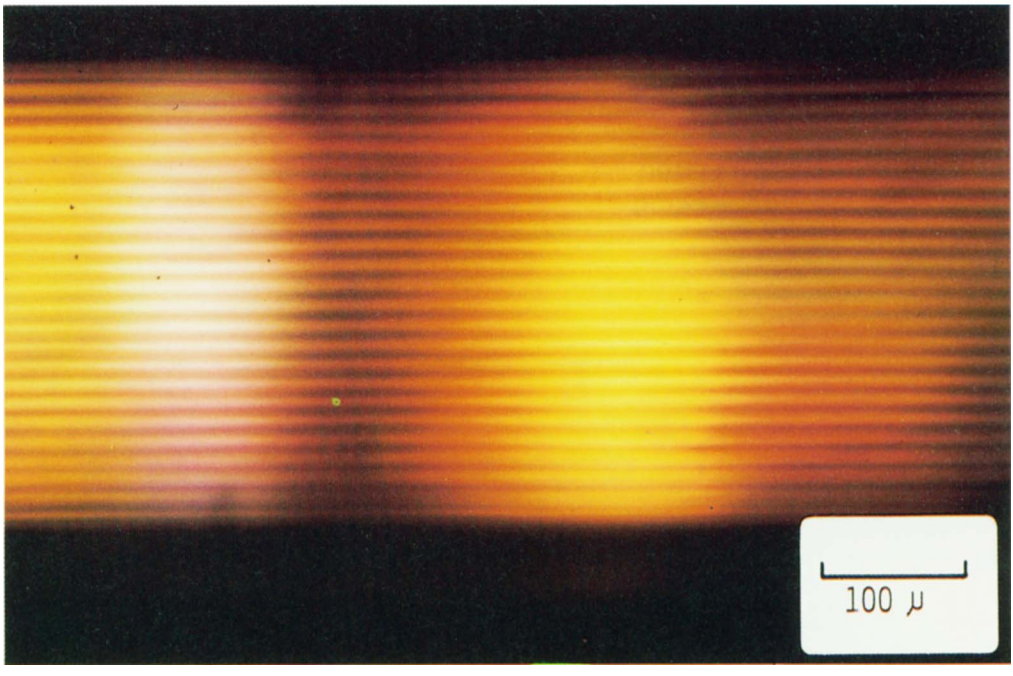

(2)

Figure 5. Room temperature polarized photomicrographs of a lyophase consisting of 0·144 volume fraction PKL in tetramethylurea. The cuvette is as in figure 2 with $z = 200\,\mu$m and $x = 2$ mm. 1 and 2 correspond to figures 4-1 and 4-2, respectively. The PKL used is a subsequent batch to that described [26], also having a broad molecular weight distribution but which is chemically more pure [56].

a 10 μm cell. The cell thickness is thus less than half of the cholesteric pitch. Note that even after short times, cf. figure 6-1, the morphology is distinctly different from that of a bulk material, cf. figure 3. At long times, a dark featureless polarized micrograph is obtained, cf. figure 6-3, since for homeotropic alignment the direction of viewing is now along one of the principle optical axes. The fact that the picture is not completely black reflects artifacts such as light levels, exposure times and imperfect polarizers. The important feature is the lack of structure. Admittedly not all experiments led to such defect free morphologies. Figure 6-4 shows the same solution in a 100 μm thick cell after long times. The thickness is about four times the cholesteric pitch. Note here that the morphology is neither that of bulk solution, cf. figure 3, or homeotropic alignment, cf. figure 6-4. Wall effects can thus be assumed to be operative but not dominant.

The pitch properties of cholesteric phases, also referred to as twisted nematics, are sensitive to choice of solvent, concentration and temperature [5, 32]. Simple considerations of the temperature and concentration dependence of the pitch in terms of a dilution model, however, do not account for the entire measured effect. The discrepancy is thought to reflect conformational changes of the pendant side chains in polyaminoacids. The temperature dependence of the pitch for PKL is shown in figure 7. Its dependence is somewhat larger than that usually found for PBLG [33]. The concentration dependence of the cholesteric pitch is demonstrated by the photomicrograph in figure 8. A concentration gradient leads to a gradient in the pitch. This is discernable as a colour change from green to red in the photomicrograph of the sample as the cholesteric line spacing varies through the wavelength of visible light, 0·5–0·6 μm. At a particular combination of temperature, concentration and solvent the pitch becomes infinite, indicating that the twist angle between adjacent molecules is zero, giving rise to a nematic phase singularity referred to as a compensated cholesteric phase. The sense of the cholesteric twist can thus be varied by varying these independent experimental parameters in the vicinity of those required to produce the compensated cholesteric structures, however, the twist angle between adjacent molecules is only a fraction of a degree.

This discussion is devoted to lyotropic cholesteric phases and reflects the lack of data regarding wall alignments for thermotropic nematic polymers. Such materials are currently of interest in connection with their potential, commercial applications and studies to reveal their wall behaviour will no doubt be forthcoming. From theoretical considerations, however, Meyer [34] has rationalized that without specific interactions the director ought to be parallel to the wall. This has been shown to be true for poly(*p*-benzamide), a lyotropic nematic polymer [35].

Evidence of wall effects in polymer rheology have not been extensively investigated due presumably, in part, to the lack of simultaneous rheological and optical studies. Experiments on low molar mass liquid crystals, however, give every reason to expect a considerable effect under the right circumstances. We might argue that the wall propagation length would scale with the persistence length of the polymeric liquid crystal chain. Capillary flow of a low molar mass nematic with perpendicular wall orientation [36] for example, was shown to be highly dependent on capillary diameter and shear rate, in agreement with Currie's model [22]. Parallel plate flow for a low molar mass smectic [10] and a nematic polymer [37] with homeotropic alignment was found to be characterized by a yield stress. For the smectic material it was highly dependent on the number of defects. A well-aligned sample was more prone to flow since the smectic planes could slide over one another. Defects as manifested by increased birefringence were accompanied by increased shear and yield stresses.

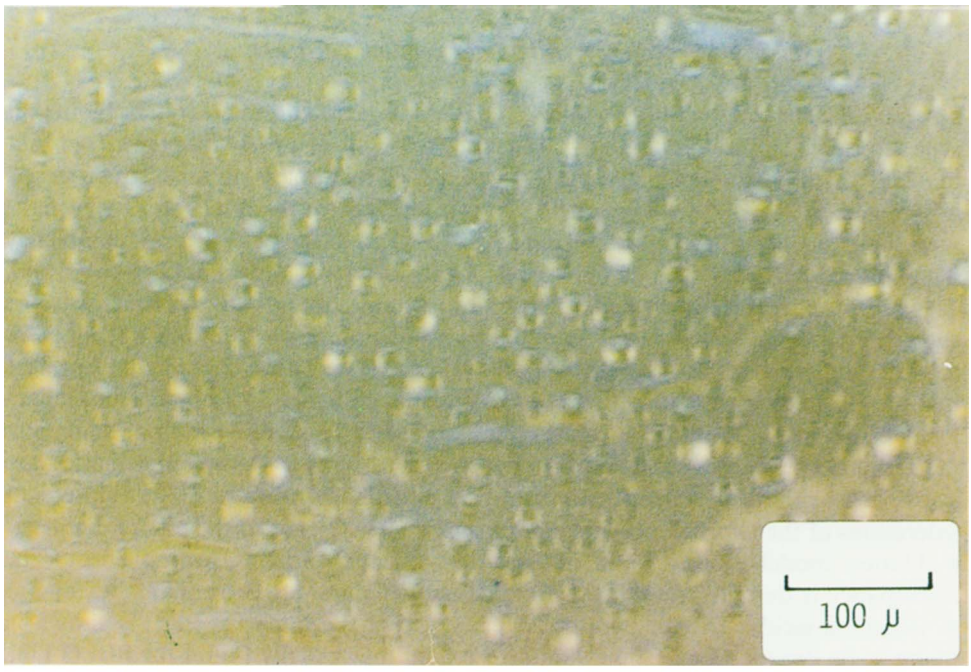

(1)

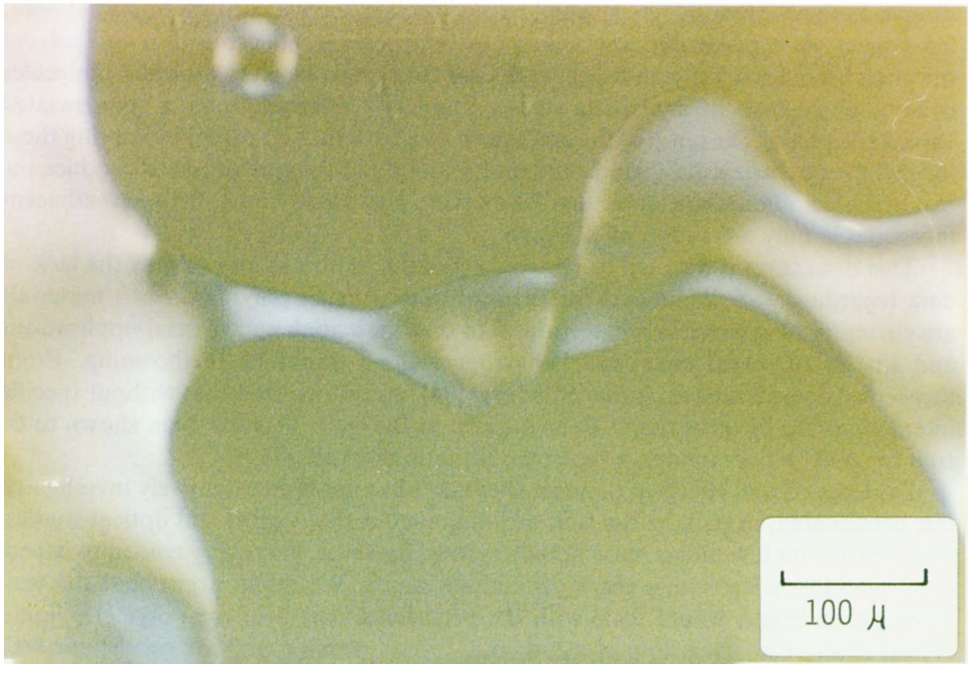

(2)

Figure 6. Room temperature polarized photomicrographs showing the time evolution of homeotropic orientation in a 10 μm cell for a PKL lyophase in tetrahydrofuran. The volume fraction, Φ, is 0·134. (1) after 1/2 hour, (2) after 5 hours and (3) after 5 days. (4) Shows the same sample after 7 days for a 100 μm cell. The PKL sample is as in figure 3.

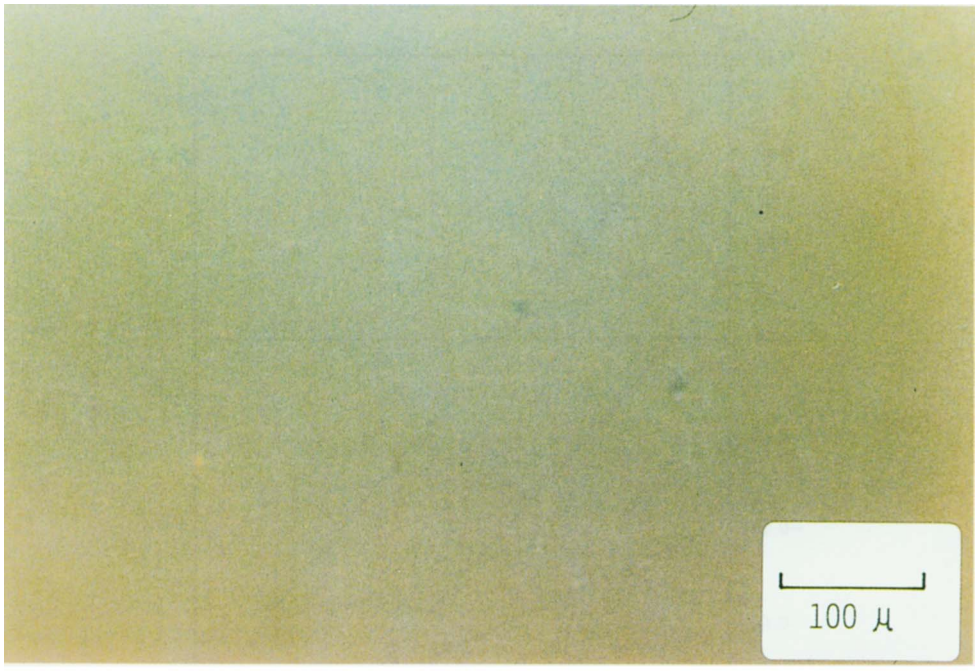

(3)

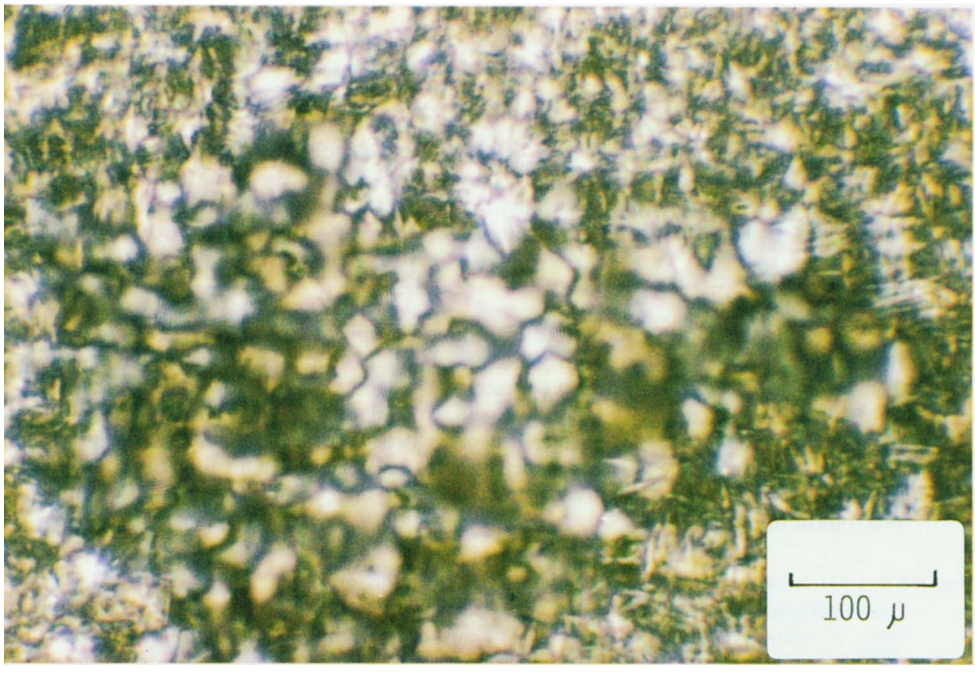

(4)

Figure 6 (*continued*).

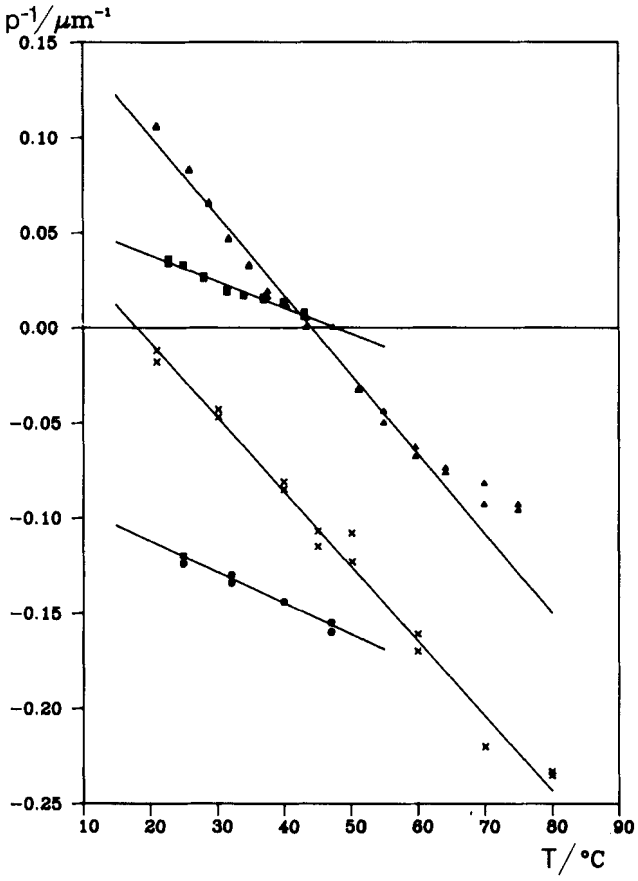

Figure 7. The temperature dependence of the reciprocal cholesteric pitch, P, for PKL lyophases using material as in figure 5. The solvents and volume fractions, Φ, are cyclohexanone (●) $\Phi = 0{\cdot}22$, tetrahydrofuran (■) $\Phi = 0{\cdot}16$, tetramethylurea (▲) $\Phi = 0{\cdot}159$, is isophorone (3,5,5-trimethyl-2-cyclohexen-1-one) (x) $\Phi = 0{\cdot}195$.

Figure 8. A room temperature polarized photomicrograph of a PKL/TNF charge-transfer lyophase in tetrahydrofuran having thickness 16 μm exhibiting a concentration gradient. The upper right is dark indicating the pitch, P, is greater than the wavelength of visible light, the centre is red indicating $P \approx 0{\cdot}6\,\mu$m and the lower left is green indicating $P \approx 0{\cdot}5\,\mu$m. Material as in figure 5. It is noteworthy that a lyophase does form for the ternary system: solvent, polydonor, acceptor. It had been thought likely that the interactions involved would greatly decrease the polymer solubility possibly leading to precipitation.

Figure 9. (1) A room temperature polarized photomicrograph of an interpenetrating two phase network of PKL lyophase in isotropic tetramethylurea solution for a 200 μm thick sample; volume fraction, Φ, is 0·245. The amount of lyophase is much less than that of isotropic phase and is present in the form of permeating mesophasic arms. Material as in figure 5. (2) A room temperature polarized photomicrograph of an interpenetrating two phase network of PKL lyophase in isotropic dimethylacetamide solution for a 100 μm thick sample; $\Phi = 0{\cdot}184$. Note that in contrast to 1, the lyophase predominates forming polygons with mesophase in the perimeters. The interior of the polygons is composed of isotropic phase. Material as in figure 3.

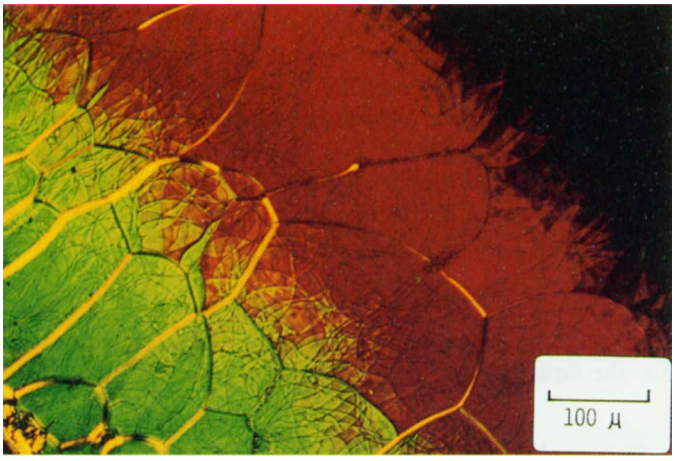

Figure 8

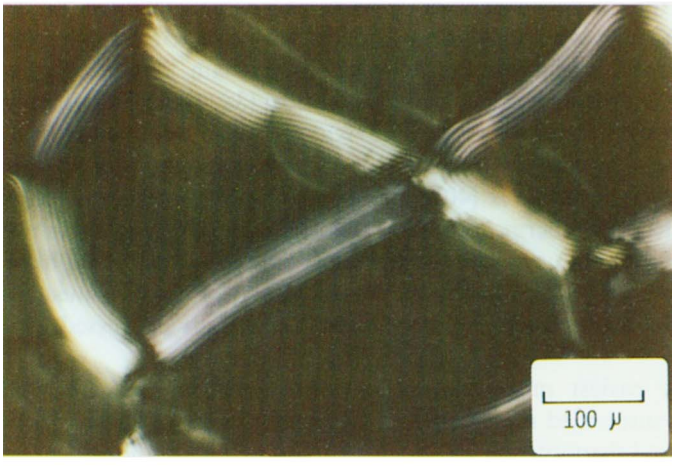

(1)

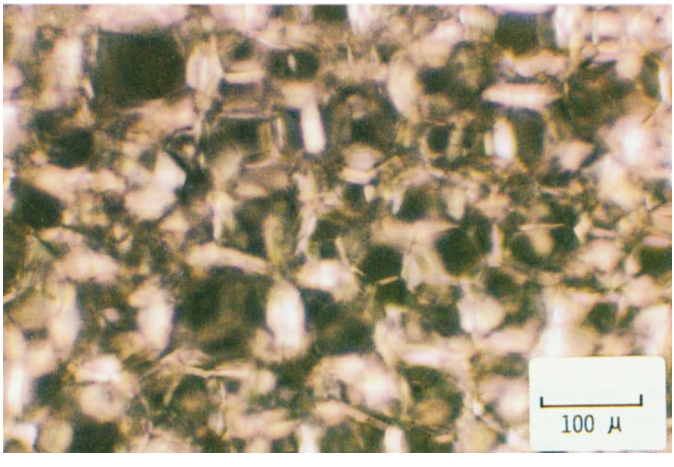

(2)

Figure 9

Wall effects could have appreciable influence in industrial processing of liquid-crystalline polymers since processes often force the molten polymer through small orifices. When the dimensions of such orifices become less than twice the propagation length for wall alignment, effects are to be expected. Processes of potential interest in this regard can include extrusion coating, film extrusion, injection moulding and fibre spinning. Monofilaments containing 1 g material per 10 km fibre are routinely produced, i.e. a diameter of 10 μm. This is of course well below twice the propagation lengths mentioned previously even when taking post-extrusion draw down into account.

Wall effects will also be effected by the geometries of the constricted orifices encountered in any given process and their relationship to the bend, twist and splay elastic moduli for the liquid crystal polymer in question.

(*b*) *Effect of coexisting multiphases*

A complicating factor in describing the rheology of liquid-crystalline polymers is the possibility for the coexistence of up to three phases: isotropic, liquid-crystalline and crystalline. The apparent inconsistency with the Gibbs phase rule can be explained by the fact that polymers can exhibit chain length polydispersity and compositional heterogeneity. Extensive theoretical [38–41] and experimental [42, 43] studies have been performed on lyotropic rigid rod polymers to elucidate equilibrium phase behaviour between isotropic solution and mesophase; and even isotropic solution and two mesophases [40]. Chain length polydispersity is shown to have considerable effect. For thermotropic copolyesters, in addition to chain polydispersity, there is the additional question of compositional heterogeneity. Biphasic behaviour for thermotropic polyesters has in fact been noted [44, 45]. Unusual rheological properties might be expected for thermotropic materials processed in the biphasic region.

One of the easiest morphologies to understand is the case where isolated spherulites are suspended in a matrix of isotropic material. These will be formed in both lyotropic and thermotropic mesophases in the vicinity of the critical concentration and clearing temperature, respectively. This morphology was recognized already in 1933 for low molar mass lyotropic materials [46], and has also been observed for polymers, especially PBLG, for which it has been extensively studied [29, 47].

In studies of PKL in this work, another morphology of biphasic mesophase-isotropic solution was observed as shown in figure 9-1. This morphology consists of two interpenetrating phases, i.e. cholesteric lyophase and isotropic solution. Of special interest is that the lyophase is continuous even though it is only present in

Figure 10. A room temperature polarized photomicrograph of a PKL lyophase showing both spherulites and fingerprint cholesteric phase. The spherulites are presumably a lyophase but in principle could be crystallines. The solvent is cyclohexanone, thickness 50–100 μm and the volume fraction, Φ, is 0·200; material as in figure 5.

Figure 11. Room temperature photomicrographs of a PKL/TNF charge-transfer complex lyophase showing the coexistence of three phases. The solvent is isophorone, the volume fraction, Φ, is 0·134 and the thickness is 100 μm; material as in figure 5. (1) polarized, showing the three phases: isotropic, bulk liquid crystal texture and spherulites. (2) unpolarized, showing the concentration from the yellow colour intensity: spherulite > bulk liquid crystal phase > isotropic.

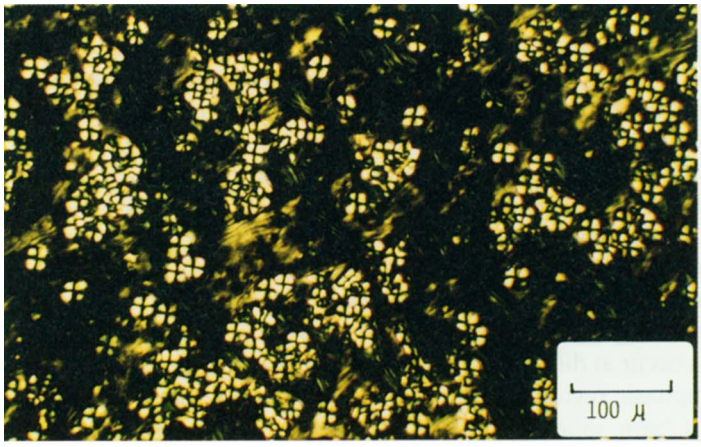

Figure 10

(1)

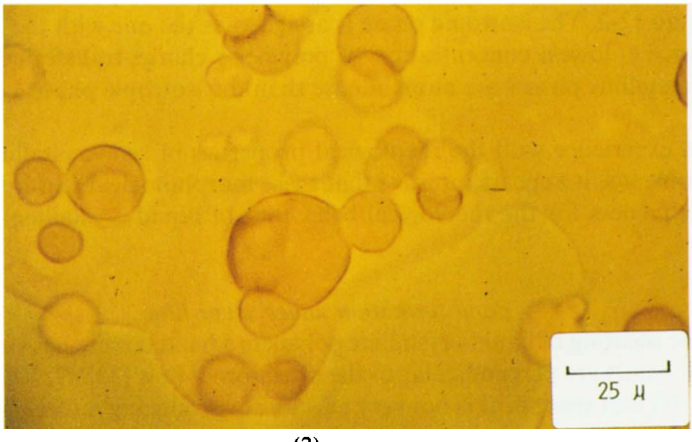

(2)

Figure 11

small amounts. Careful inspection reveals several cholesteric lines running parallel to the arms of the penetrating lyophase. Such a morphology has been proposed [42] based on electron micrographs in the wide biphasic region of the phase diagram for PBLG. It was further suggested that the interpenetrating nature of the morphology gave rise to a mechanically self-supporting gel.

Under other experimental conditions, this morphology can be obtained in a modified form, as shown in figure 9-2, where the biphasic nature is dominated by the anisotropic phase. This morphology is characterized by polygons with anisotropic perimeters and isotropic cores. Close examination of the original photographs, show the occasional occurrence of a few cholesteric striations in the polygon perimeters. Such a morphology has been reported previously for PBLG [48]. Since the planes of the polygons occur at different sample depth, focusing is an arduous task. Progressing out of the biphasic region to an all anisotropic regime, a polymorphic morphology consisting of both spherulites—and the focal conic or fingerprint texture can be observed, as shown in figure 10. It is not known whether these two polymorphs are kinetic artifacts or represent distinct phases resulting from, for example, fractionation by molecular weight.

Systems containing three polymorphs have also been observed. Lyotropic phases of the charge-transfer complex of PKL with 2,4,7-trinitro-9-fluorenone, TNF, were investigated with regard to their photoconductivity, i.e. the original motivation for this work [26, 27]. Figure 11-1 is a photomicrograph showing the coexistence of three phases, i.e. isotropic, spherulitic and bulk liquid crystal phase. The charge-transfer complex has a characteristic yellow-orange color enabling the relative phase concentrations to be determined qualitatively by visual inspection of the unpolarized photomicrographs as seen in figure 11-2. The concentration in the three phases was seen to be: spherulites > bulk liquid crystal > isotropic. Considering the broad molecular weight distribution of the polymer utilized in these experiments, a fractionation is considered likely to have occurred.

Figure 12-1 shows a similar system for which there is isotropic, bulk liquid crystal phase and wall oriented pseudo-isotropic phase (homeotropic or random planar). The pseudo-isotropic nematic phase and the isotropic phase can be distinguished by the different intensities of the yellow colour in the unpolarized photomicrographs, as shown in figure 12-2. The isotropic phase is assigned as the one with the least intense yellow colour, i.e. lowest concentration of polymeric charge-transfer complex. The two liquid-crystalline phases are more intense than the isotropic phase and similar in colour.

Based on experience with the rheological properties of semicrystalline polymers and polymer blends, it appears intuitive that these morphological features must have serious consequences for the rheological behaviour of liquid-crystalline polymers.

(*c*) *Band formation under shear flow*

During the shearing of liquid-crystalline polymers a band texture has been observed for which the bands are perpendicular to the direction of flow [38, 49, 50]. It has been pointed out [38] that shear flow is not very effective in producing molecular alignment and the disorientation or angle between the long molecular axis and the flow direction can remain quite high, 30°, even at moderate rates of shear, $\dot{\gamma}$ of $50\,s^{-1}$. Additional orientation accompanied by the formation of bands is achieved during relaxation after the cessation of flow. The individual molecules for a case in point have been

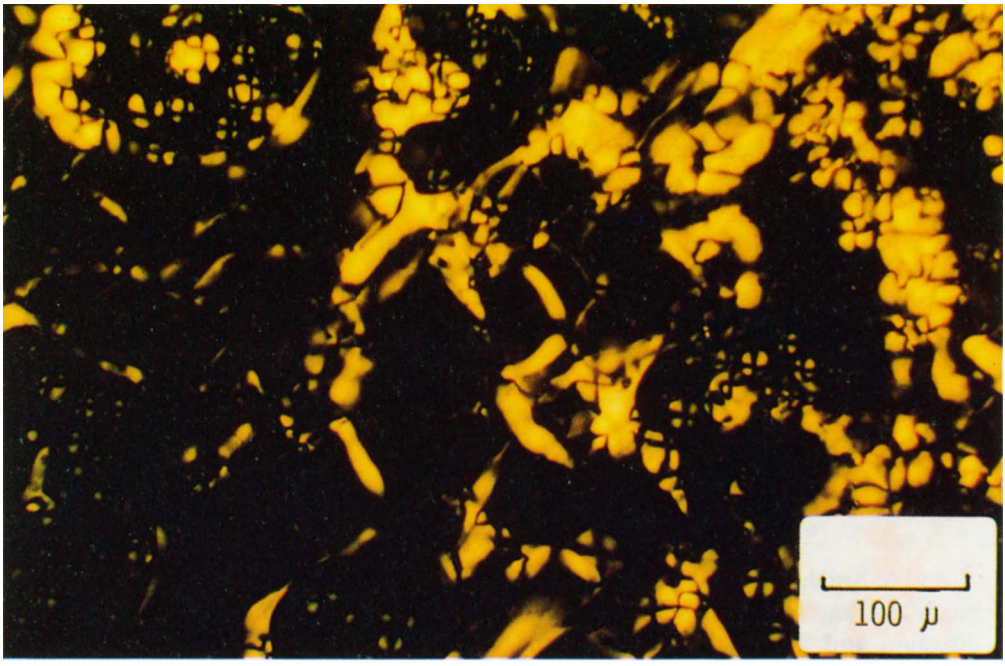

(1)

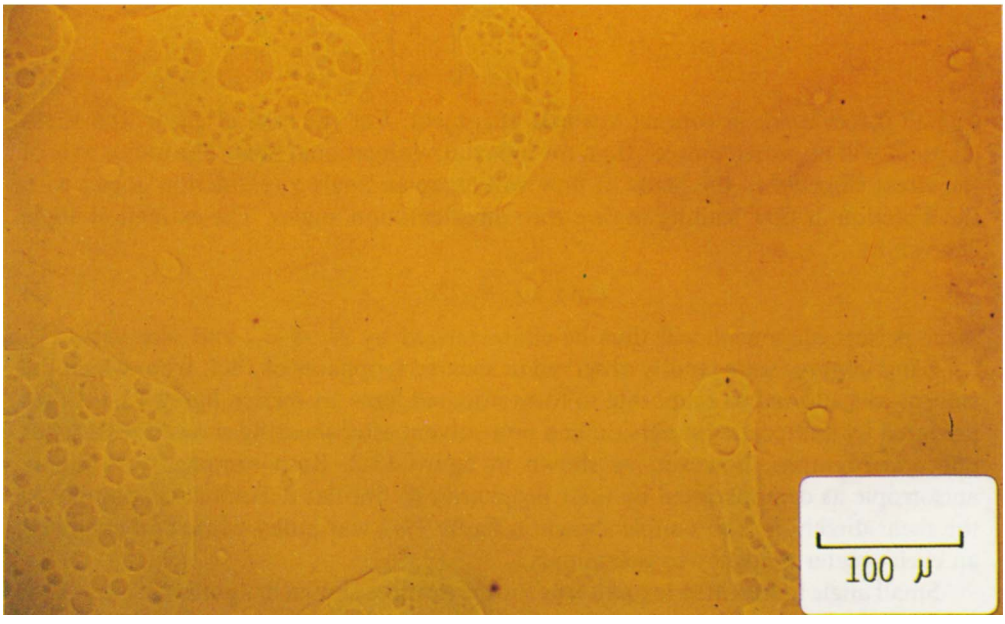

(2)

Figure 12. As in figure 11 but in tetrahydrofuran. (1) polarized, showing the two phases: isotropic, bulk liquid crystal phase and pseudo-isotropic (homeotropic or random planar). (2) unpolarized, showing the concentration from the yellow colour intensity. The intensities of the pseudo-isotropic and spherulitic textures are comparable to that of the bulk liquid crystal texture. The intensity of the isotropic phase is considerably less than that for the anisotropic phase.

shown [49] to lie between 0° and ± 36° in a sinusoidal fashion giving rise to the banded structure. Attempts have been made to attribute the formation of bands to flow instabilities [51] and negative normal stresses [52].

The complications resulting from modelling uniaxial orientation under conditions of shear flow have been discussed [4, 53]. The stress field takes the form:

$$\sigma = \begin{pmatrix} \sigma_{11} & \sigma_{12} & 0 \\ \sigma_{12} & \sigma_{22} & 0 \\ 0 & 0 & \sigma_{33} \end{pmatrix}$$

$$= \begin{pmatrix} \sigma_{33} & 0 & 0 \\ 0 & \sigma_{33} & 0 \\ 0 & 0 & \sigma_{33} \end{pmatrix} + \begin{pmatrix} N_1 + N_2 & \sigma_{12} & 0 \\ \sigma_{12} & N_2 & 0 \\ 0 & 0 & 0 \end{pmatrix}. \quad (1)$$

where

$$N_1 = \sigma_{11} - \sigma_{22}, \quad N_2 = \sigma_{22} - \sigma_{33}.$$

N_1 and N_2 are the first and second normal stress differences, respectively; $-N_2$ is often much less than N_1. The σ subscripts refer to an orthogonal frame where 1 is the flow direction and 2 is the direction of the gradient. The σ_{11} term is thus given by $N_1 + N_2 \sim N_1$, i.e. the normal stress difference which tends to tip the molecules out of the flow direction. This is in contrast to the case for elongational flow where

$$\sigma = \begin{pmatrix} \sigma_{11} & 0 & 0 \\ 0 & 0 & 0 \\ 0 & 0 & 0 \end{pmatrix} \quad (2)$$

and all forces work in concert towards alignment. For the case of shear, the stress ellipsoid will be more complex than for uniaxial, elongational flow. The major axis of the stress ellipsoid in the plane of flow will make an angle χ (extinction angle) with the direction of flow leading to non-zero disorientation angles. The extinction angle is given by

$$\tan\chi = N_1/2\sigma_{12}. \quad (3)$$

Near perfect alignment will thus be characterized by $N_1 \ll \sigma_{12}$ and vice versa [1].

Band textures were readily observed in sheared lyophases of PKL from which the solvent was allowed to evaporate to form oriented films, as seen in figure 13-1. Films prepared by immediate immersion in a non-solvent after shearing showed textureless photomicrographs, however, as shown in figure 13-2. Both samples were highly anisotropic as demonstrated by their propensity to fibrillar delamination parallel to the shear direction. The sample shown in figure 13-2 was milky-white and exhibited an even greater tendency to delaminate.

Small angle light scattering patterns for the samples shown in figures 13-1 and 13-2 are shown in figures 14-1 and 14-2, respectively. The scattering patterns, though not identical, both show broad ellipsoids across the equator as would be expected for a uniaxially oriented sample. For the sample with the band texture, cf. figure 13-1, the bands are perpendicular to the flow direction so the additional weak meridianal scattering for this sample shown in figure 14-1 could have its origins in the band structure and not the orientation of the individual molecules.

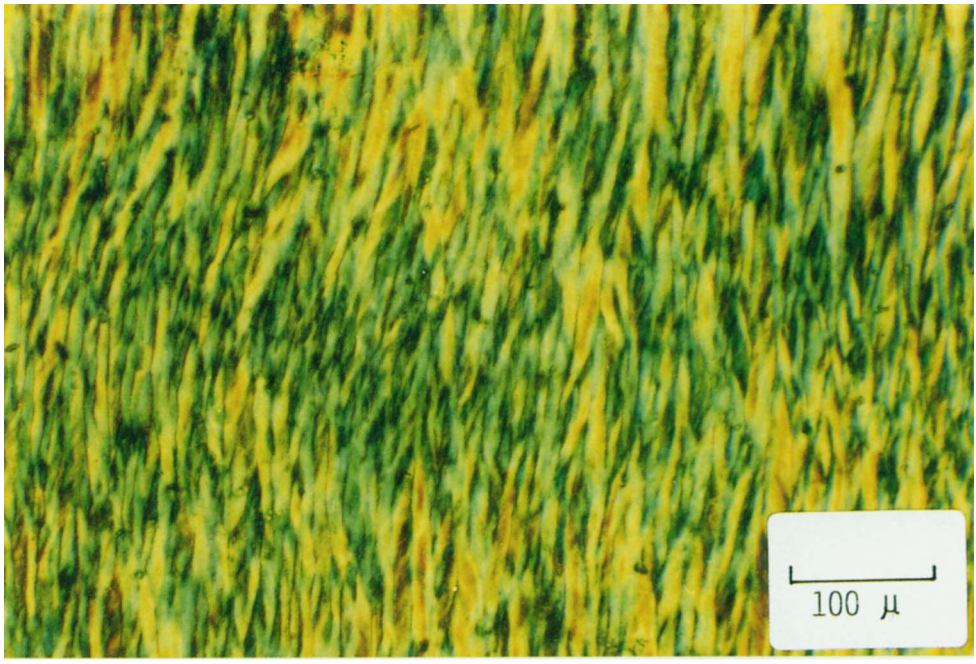

(1)

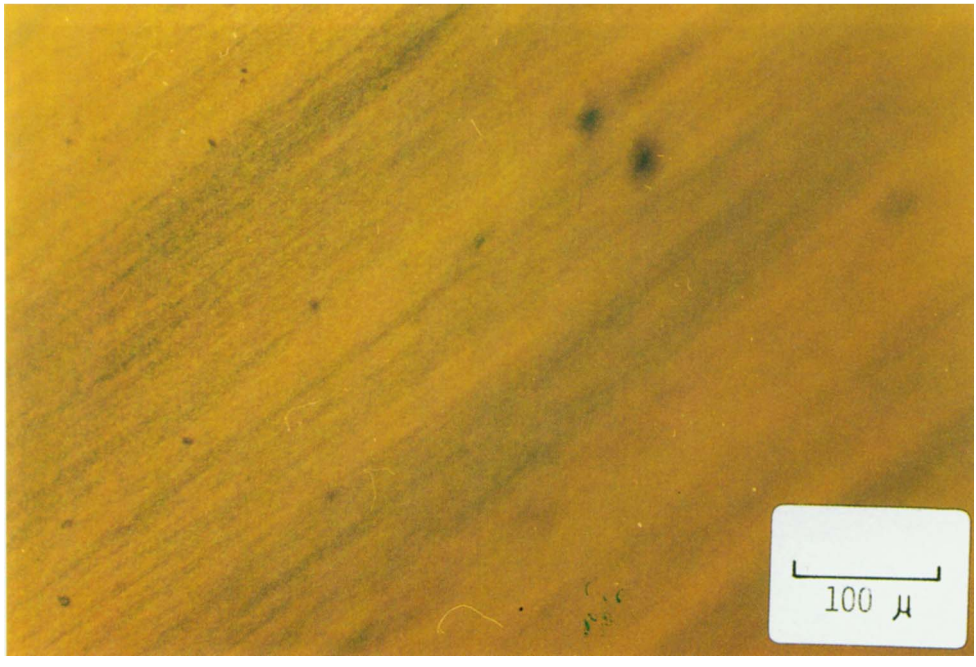

(2)

Figure 13. Room temperature photomicrographs for highly oriented PKL 10 μm films prepared from mechanically aligned lyophases with volume fraction, $\Phi = 0{\cdot}20$. Material as in figure 5. (1) A banded texture resulting from the free evaporation of tetrahydrofuran from the lyophase. (2) A textureless morphology resulting from the immersion of a PKL/tetrahydrofuran lyophase in an ethanol bath.

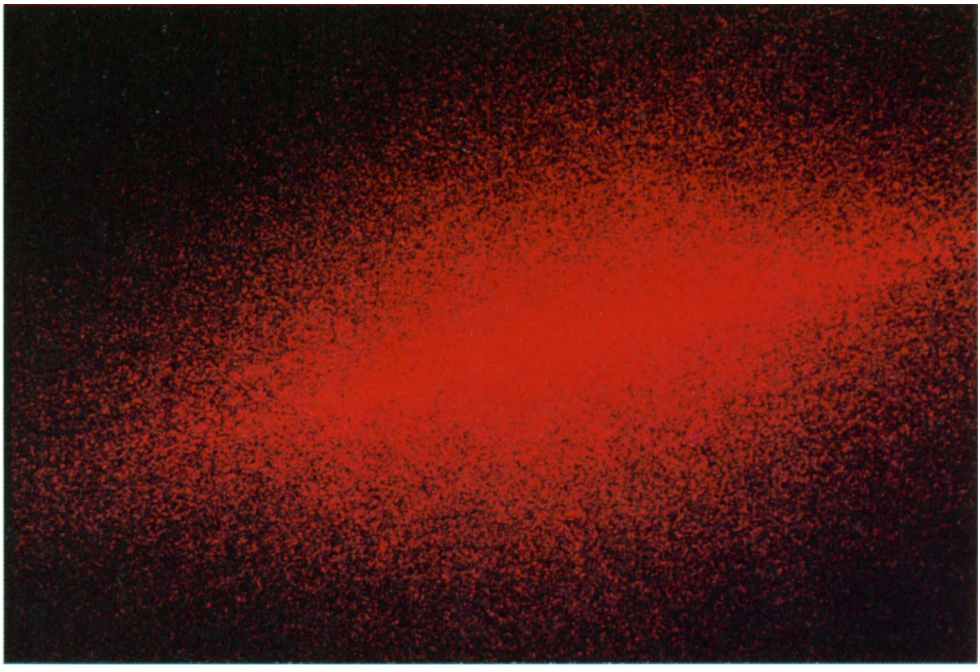

(1)

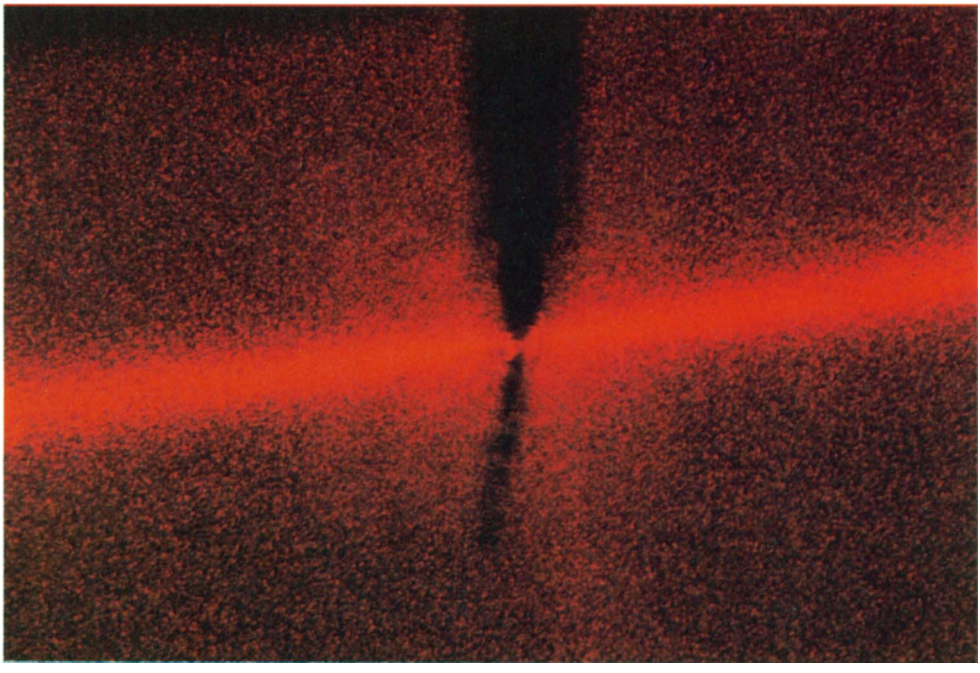

(2)

Figure 14

(*d*) *Magnetic field alignment and subsequent relaxation*

In contrast to PBLG [6, 54, 55], PKL lyophases have a negative diamagnetic anisotropy. The requirement, therefore that the long molecular axes be perpendicular to the magnetic field, **H**, is satisfied by a monodomain cholesteric phase for which the cholesteric helical axis is parallel to **H**. A photomicrograph of such a monodomain cholesteric is shown in figure 15-1; **H** is in the plane of the photograph and perpendicular to the cholesteric lines. The effect of **H**, is therefore to transform a polydomain cholesteric phase to a monodomain cholesteric phase. This is quite a different process to that involved in the magnetic field alignment of PBLG for which the diamagnetic anisotropy is positive and the effect of **H** is to transform a polydomain cholesteric to a monodomain homeotropic nematic. Rotation of **H** by 90° leads to a photomicrograph as shown in figure 15-2. Here, **H** is normal to the photograph and the polarized micrograph is featureless and invariant with respect to sample rotation. This is a consequence of the random planar orientation corresponding to a limiting order parameter, $\langle P_2 \rangle$ of $-1/2$. This is a pseudo-isotropic state and a natural consequence of the negative diamagnetic anisotropy.

This novel result opens the possibility of making nuclear magnetic resonance measurements on the cholesteric phase. Relaxation of the monodomain cholesteric to the polydomain cholesteric can be observed by removing a sample corresponding to figure 15-2 from the magnet and observing it under the microscope as a function of time as seen in figures 15-3, 15-4 and 15-5. Domains reappear after a few minutes, followed by the retardation lines, after which the equilibrium structure is reformed in about 30 minutes. This seems unusually long considering that the samples are viscous liquids which can easily be made to flow in a test tube. It has previously been reported [54, 55], however, that the morphological relaxation as measured optically is very slow, especially when compared to the time scale of viscoelastic relaxation [4, 54, 55].

(*e*) *Rheological responses and relaxations*

The rheological responses of PKL lyophases were measured on a rheometrics mechanical spectrometer and are characterized by the morphological uncertainties as noted previously; see figure 16-1. The shear stress decreases slightly by a factor of five as the shear rate, $\dot{\gamma}$, increases from $0{\cdot}015\,s^{-1}$ to $0{\cdot}6\,s^{-1}$ and then increases by a factor of two as $\dot{\gamma}$ is increased from $0{\cdot}6\,s^{-1}$ to $10\,s^{-1}$. These seem to be based on reasonable approximations of pseudo-steady state measurements as the shear rate is increased. The first few minutes of shearing at the low shear rates gave very irreproducible behaviour presumably due to the morphological changes being undergone. The results described later represent some general features which permeated the experiments without trying to over-interpret all of their peculiarities. The near constancy of shear

---

Figure 14. Small angle light scattering results for the oriented films shown in figures 13-1 and 13-2. (1) Scattering from the sample shown in figure 13-1. The scattering is concentrated in an ellipsoid across the equator compatible with the orientation direction and results from the uniaxial orientation of individual molecules. The additional weak meridianal scattering could have its origins in the band texture. (2) Scattering from the sample shown in figure 13-2. The scattering is concentrated in an ellipsoid across the equator compatible with the orientation direction as would be expected for a highly oriented uniaxial solid. The dark region is simply a masking of the primary beam. Both figures show the V_v pattern with parallel polarizers. H_v patterns with crossed polarizers are similar, but of weaker intensity.

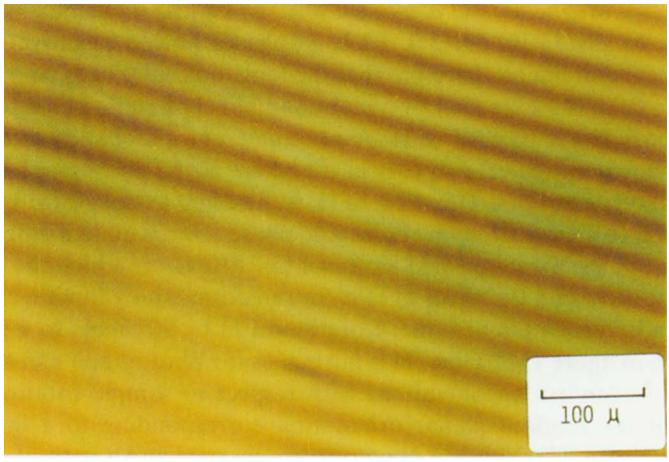

(1)

(2)

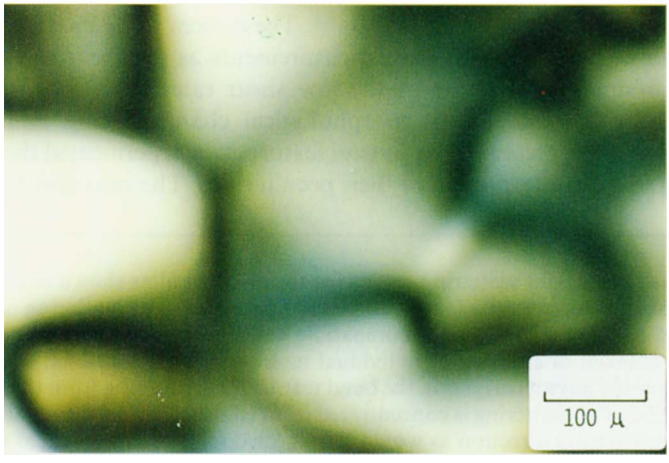

(3)

Figure 15

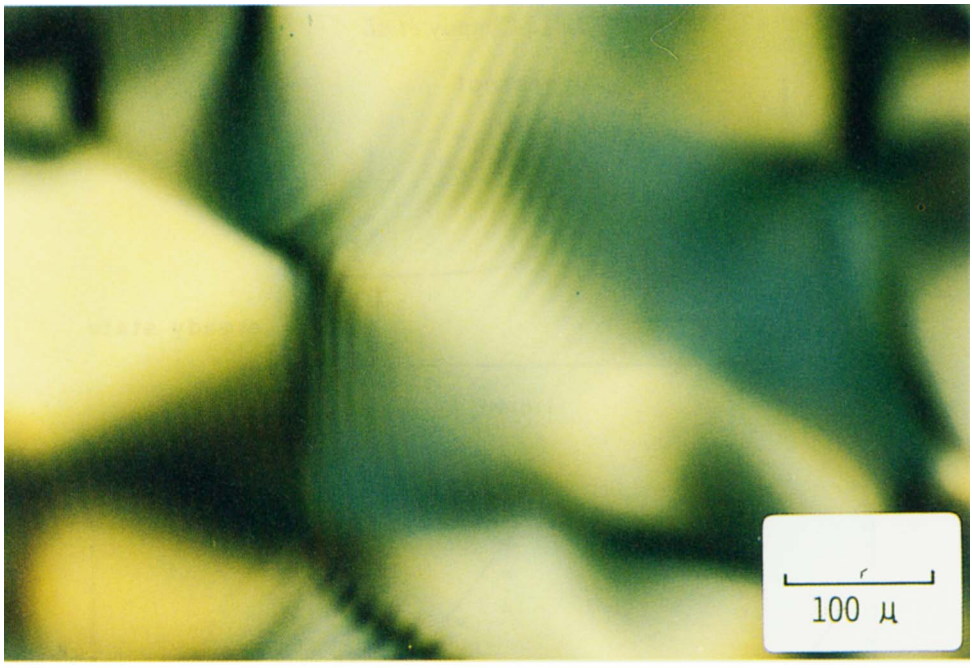

(4)

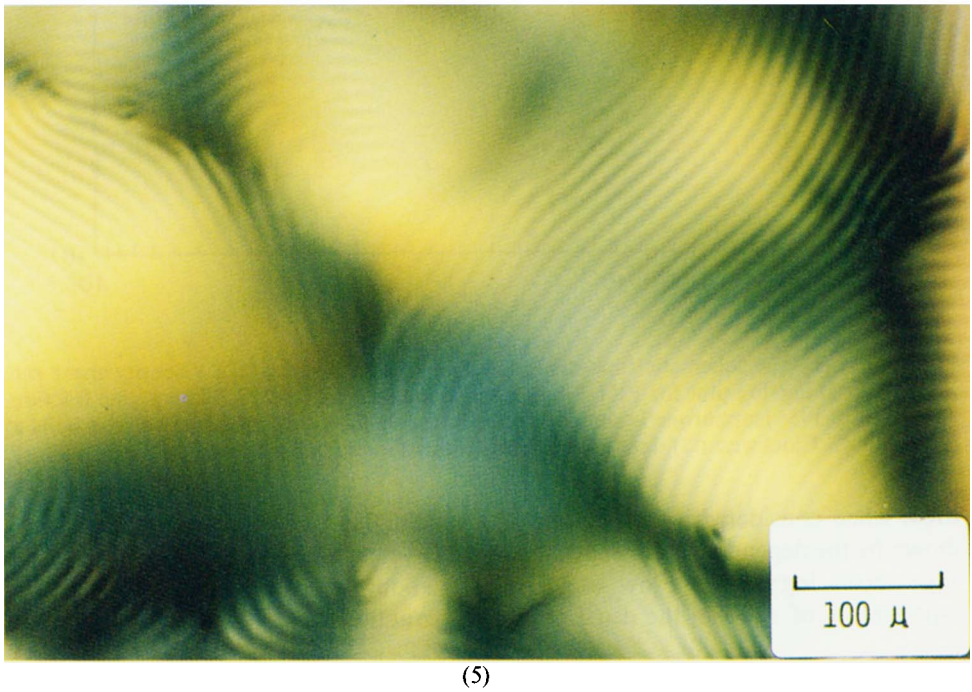

(5)

Figure 15. Room temperature polarized photomicrographs of a PKL lyophase in tetrahydrofuran which have been magnetically aligned. The thickness is 1 mm and the volume fraction, $\Phi = 0{\cdot}107$, $\mathbf{H} = 1{\cdot}2\,T$. (1) The magnetic field is in the plane of the photograph at an angle of 15° from the picture axis. The cholesteric lines are perpendicular to **H**. The time required to achieve equilibrium is 36 hours. (2) **H** is perpendicular to the plane of the photograph. (3) As (2) 5 min after removal from the magnetic field. (4) As (3) after 7 min. (5) As (3) after 30 min.

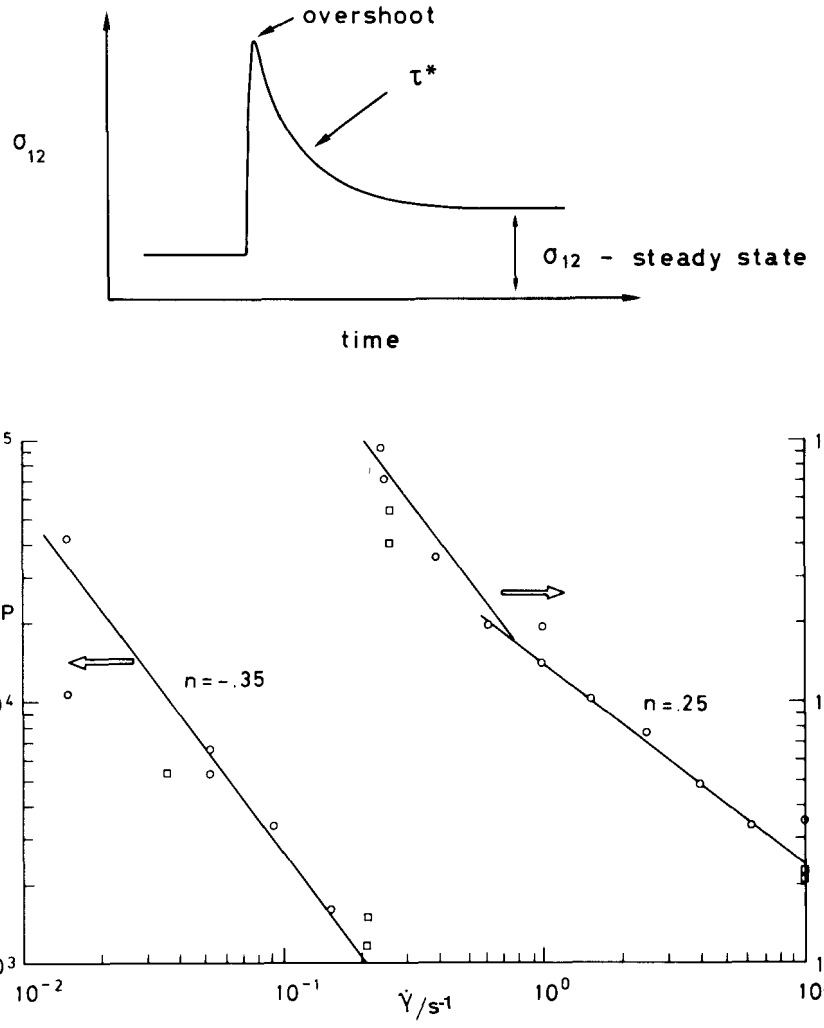

Figure 16. (1) The schematic time dependence of the shear stress. (2) Viscosity-shear rate ($\eta - \dot{\gamma}$) log–log plot for PKL lyophase in isophorone at 40·9°C. The volume fraction, $\Phi = 0{\cdot}195$. Isophorone is suitable for such rheological measurements since it boils at 220° C. Clockwise (□) data are denoted from counterclockwise data (○).

stress when considered as a function of $\dot{\gamma}$ gave highly pseudo-plastic behaviour as shown by the dependence of viscosity, η, on shear rate in figure 16-2. The slope of the $\log\eta$ versus $\log\dot{\gamma}$ plot at low values of $\dot{\gamma}$ is about $-1{\cdot}3$ indicating a power law exponent, n, of $-0{\cdot}3$ in the usual power law equation

$$\sigma = K\dot{\gamma}^n, \tag{4}$$

$$\eta = K\dot{\gamma}^{n-1}. \tag{5}$$

Power law exponents are usually positive quantities.

There was no tendency towards the establishment of a newtonian region at low values of $\dot{\gamma}$. Fluids exhibiting such yield stress behaviour are usually described by the

Bingham equation

$$\sigma = A + B\dot{\gamma}, \tag{6}$$

$$\eta = \frac{A + B\dot{\gamma}}{\dot{\gamma}}, \tag{7}$$

where A is the yield stress and $B = \eta$ for $A \to 0$. The origin of the yield stress is thought to be related to morphological changes in response to the application of the stress field.

Figure 16 shows a knee in the curve at $\dot{\gamma}$ of $0{\cdot}6\,s^{-1}$ after which the slope flattened out to become $-0{\cdot}75$, i.e. $n = 0{\cdot}25$, still a very pseudo-plastic material. In the power law context, the knee was interpreted as being indicative of a morphological transition. Polydomain structure has been shown to exist even after extensive sample shearing [4]. In the context of the Bingham equation the knee could well be an artifact of fitting two straight lines to a curve since the slope for this model on a $\log\eta - \log\dot{\gamma}$ basis varies continuously from -1 at $\dot{\gamma} \to 0$ to 0 at $\dot{\gamma} \to \infty$. Since the model does not allow for a slope < -1 (see the appendix), this example requires a model predicting an even more severe dependence of η on $\dot{\gamma}$ than that provided by the Bingham equation.

After these initial difficulties, progression to higher rates of shear was accompanied by stress overshoot followed by relaxation to a pseudo-steady state shear stress which was used to calculate the steady state viscosity in figure 16-2. The fact that the steady state shear stress did not vary extensively during the course of the experiments might indicate that the system was prone to relax to a yield stress level (the pseudo-steady shear stress value) which the material was capable of supporting. This value was always between 10 and 50 per cent of the peak value for the loading pattern employed.

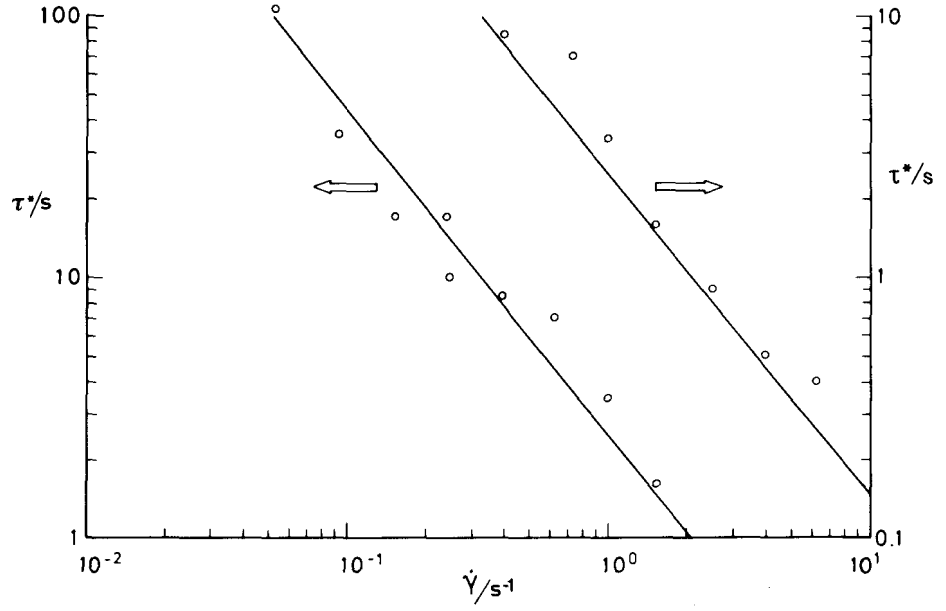

Figure 17. Relaxation time, τ^*, for stress overshoot as a function of shear rate $\dot{\gamma}$. Details are as in figure 16.

The relaxation time, τ^*, associated with the overshoot decreased with increasing shear rate as shown in figure 17;

$$\tau^* \alpha \dot{\gamma}^{-1\cdot 2}. \tag{8}$$

The relaxation of shear stress after the cessation of shearing required the order of a few seconds and was independent of shear rate. These relaxation times are appreciably shorter than those observed optically for domain formation in Section 2D as reported previously [4]. Samples which were allowed to stand without shearing for ca. 1/2 hour exhibited enhanced stress overshoot when subject to renewed shearing, but the steady state shear stress was comparable to that measured previously. The enhanced overshoot is thought to reflect the regeneration of complicated domain structure in the sample. There are reports for lyotropic liquid-crystalline polyaminoacids which are racemic and therefore nematic which are to the contrary: the overshoot peak becomes smaller with increasing time of rest [58, 59].

3. Conclusion

We have presented evidence for a wide variety of differing morphologies that a lyotropic polyaminoacid, poly-[N^{ε}-(9-carbazolyl-carbonyl)-L-lysine], PKL, is capable of assuming and we have tried to rationalize the expected consequences for the rheological behaviour. The many morphological modifications which can be obtained imply that the mechanical properties of thermotropic liquid-crystalline polymers will be strongly influenced by their thermal and processing histories.

The authors would like to thank J. Halstrøm and K. Kovacs, both no longer with the group, for generously supplying samples of PKL with which this work was carried out. They would also like to thank F. E. Andersen for assistance with the rheological measurements. The authors would also like to thank Istituto G. Donegani for defraying the publication costs of this article.

Appendix

The slope, m, of the $\log\eta - \log\dot{\gamma}$ representation of the Bingham equation is obtained by differentiating $\log\eta$, (7), with respect to $\log\dot{\gamma}$. Thus

$$\log\eta = \log\left[\frac{A + B\dot{\gamma}}{\dot{\gamma}}\right], \tag{7}$$

$$m = \frac{d\log\eta}{d\log\dot{\gamma}},$$

$$= \frac{\dot{\gamma} d\log\eta}{d\dot{\gamma}},$$

$$= \dot{\gamma}\left[\frac{\dot{\gamma}}{A + B\dot{\gamma}}\right]\left[-\frac{A}{\dot{\gamma}^2}\right], \tag{A 2}$$

$$m = -\frac{A}{A + B\dot{\gamma}},$$

being continuous and monotonic gives:

$$\lim_{\dot{\gamma}\to 0} m = -1$$

and

$$\lim_{\dot{\gamma}\to \infty} m = 0.$$

References

[1] BAIRD, D. G., 1978, *Rheology of Polymers with Liquid Crystalline Order in Liquid Crystalline Order of Polymers*, edited by A. Blumstein (Academic Press), p. 237 ff.

[2] WISSBRUN, K. F., 1981, *J. Rheology*, **25**, 619.

[3] ASADA, T., 1982, *Rheo-optical Studies of Polymer Liquid Crystalline Solutions in Polymer Liquid Crystals*, edited by A. Ciferri, W. R. Krigbaum and R. B. Meyer (Academic Press), p. 247 ff.

[4] ONOGI, Y., WHITE, J. L., and FELLERS, J., 1980, *J. Non-Newtonian Fluid Mech.*, **7**, 121.

[5] DUPRÉ, D. B., 1982, *Techniques for the Evaluation of Material Constants and the Study of Pretransitional Phenomena in Polymeric Liquid Crystals in Polymer Liquid Crystals*, edited by A. Ciferri, W. R. Krigbaum and R. B. Meyer (Academic Press), p. 165 ff.

[6] STRIDHAR, C. G., HINES, W. A., and SAMULSKI, E. T., 1974, *J. chem. Phys.*, **61**, 947.

[7] THOMAS, E. L., and WOOD, B. A., 1985, *Faraday Discuss. chem. Soc.*, **79**, 229; and the ensuing discussion, especially the contributions of F. C. Frank and A. M. Donald and the reply of E. L. Thomas and B. A. Wood.

[8] Reference 2: references therein, pp. 652–3.

[9] ASADA, T., MURAMATSU, H., WATANABE, R., and ONOGI, S., 1980, *Macromolecules*, **13**, 867.

[10] HORN, R. G., and KLÉMAN, M., 1978, *Ann. Phys.*, **3**, 229.

[11] Reference [2], references therein, p. 654.

[12] GRAZIANO, D. J., and MACKLEY, M. R., 1984, *Molec. Crystals liq. Crystals*, **106**, 73.

[13] ORNSTEIN, L. S., and KAST, W., 1933, *Trans. Faraday Soc.*, **29**, 931.

[14] LYNGAAE-JØRGENSEN, J., and SØNDERGAARD, K., 1987, *Polym. Engng Sci.*, **27**, 351.

[15] ONOGI, S., and ASADA, T., 1980, *Rheology and Rheo-optics of Polymer Liquid Crystals, in Rheology*, Vol. 1, *Principles*, edited by G. Astarita, G. Marrucci and L. Nicolais (Plenum Press), p. 127 ff.

[16] GOTSIS, A. D., and BAIRD, D. G., 1985, *J. Rheology*, **29**, 539.

[17] DUKE, R. W., and CHAPOY, L. L., 1976, *Rheol. Acta*, **15**, 548.

[18] WISSBRUN, K. F., 1980, *Brit. Polym. J.*, p. 163 ff.

[19] ASADA, T., MARUHASHI, Y., and ONOGI, S., 1979, *J. Phys., Paris* C1, **36**, 229.

[20] CHAPOY, L. L., and DUKE, R. W., 1979, *Rheol. Acta*, **18**, 537.

[21] Reference [2], references therein, p. 648.

[22] CURRIE, P. K., 1977, *Rheol. Acta*, **16**, 205.

[23] ONOGI, S., MASUDA, T., and MATSUMOTO, T., 1970, *Trans. Soc. Rheology*, **14**, 275.

[24] MATSUMOTO, T., SEGAWA, Y., WARASHINA, Y., and ONOGI, S., 1973, *Trans. Soc. Rheology*, **17**, 47.

[25] LOBE, V. M., and WHITE, J. L., 1979, *Polym. Engng Sci.*, **19**, 617.

[26] CHAPOY, L. L., BIDDLE, D., HALSTRØM, J., KOVACS, K., BRUNFELDT, K., QASIM, M. A., and CHRISTENSEN, T., 1983, *Macromolecules*, **16**, 181.

[27] CHAPOY, L. L., MUNCK, D. K., RASMUSSEN, K. H., JUUL DIEKMANN, E., SETHI, R. K., and BIDDLE, D., 1984, *Molec. Crystals liq. Crystals.*, **105**, 353.

[28] COGNARD, J., 1982, *Molec. Crystals liq. Crystals*, Suppl. **1**, 1–78.

[29] ROBINSON, C., 1956, *Trans. Faraday Soc.*, **52**, 571.

[30] HARTSHORNE, N. H., and STUART, A., 1970, *Crystals and Polarizing Microscope* (Edward Arnold), p. 538 ff.

[31] UEMATSU, Y., TOMIZAWA, J., KODOHORA, F., and SASAHI, T., 1980, *Academic Report of the Tokyo Institute of Polytechnics*, **2**, 53.

[32] CZARNIECKA, K., and SAMULSKI, E. T., 1981, *Molec. Crystals liq. Crystals*, **63**, 205.

[33] DUPRÉ, D. B., and DUKE, R. W., 1975, *J. chem. Phys.*, **63**, 143.

[34] MEYER, R. B., 1982, *Macroscopic Phenomena in Nematic Polymers in Polymer Liquid Crystals*, edited by A. Ciferri, W. R. Krigbaum and R. B. Meyer (Academic Press), p. 133 ff.

[35] PLANAR, M., and BESTE, L. F., 1977, *Macromolecules*, **10**, 1401.

[36] FISHER, J., and FREDRICKSON, A. G., 1969, *Molec. Crystals. liq. Crystals*, **8**, 267.

[37] KULICHIKIN, V. G., VASIL'YEVA, N. V., PLATONOV, V. A., MALKIN, A. YA., BELOUSOVA, T. A., KHANCHICH, O. A., and PAPKOV, S. P., 1980, *Polym. Sci. U.S.S.R.*, **21**, 1545.

[38] FLORY, P. J., 1984, *Adv. Polym. Sci.*, **59**, 1.

[39] FLORY, P. J., and ABE, A., 1978, *Macromolecules,* **11**, 1119.
[40] FLORY, P. J., and ABE, A., 1978, *Macromolecules,* **11**, 1122.
[41] FLORY, P. J., and FROST, R. S., 1978, *Macromolecules,* **11**, 1126.
[42] UEMATSU, I., and UEMATSU, Y., 1984, *Adv. Polym. Sci.,* **59**, 37.
[43] PAPKOV, S. P., 1984, *Adv. Polym. Sci.,* **59**, 75.
[44] LENZ, R. W., 1985, *Faraday Discuss. chem. Soc.,* **79**, 21.
[45] BLUMSTEIN, A., GAUTHIER, M. M., THOMAS, O., and BLUMSTEIN, R. B., 1985, *Faraday Discuss. chem. Soc.,* **79**, 33.
[46] LAWRENCE, A. S. C., 1933, *Trans. Faraday Soc.,* **29**, 1008.
[47] PATEL, D. L., and DUPRÉ, D. B., 1980, *J. Polym. Sci.,* **18**, 1599.
[48] SUBRAMANIAN, R., and DUPRÉ D. B., 1984, *J. Polym. Sci.,* **22**, 2207.
[49] VINEY, C., DONALD, A. M., and WINDLE, A. H., 1985, *Polymer,* **26**, 870.
[50] ZACHARIADES, A. E., and LOGAN, J. H., 1985, *Recent Advances in Liquid Crystalline Polymers*, edited by L. L. Chapoy (Elsevier Applied Science Publishers), p. 177 ff.
[51] MARUCCI, G., 1985, *Pure appl. Chem.,* **57**, 1545.
[52] CHAFFEY, C. E., and PORTER, R. S., 1985, *J. Rheology,* **29:3**, 281.
[53] WHITE, J. L., and DIETZ, W., 1979, *J. Non-Newtonian Fluid Mech.,* **4**, 299.
[54] SOBAJAMA, S., 1967, *J. phys. Soc. Japan,* **23**, 1070.
[55] DUPRÉ D. B., and HAMMERSMITH, J. R., 1974, *Liquid Crystals and Ordered Fluids*, Vol. 2, edited by J. Johnson and R. Porter (Plenum Press), p. 237.
[56] CLAUSEN, K., and BRUNFELDT, K., 1986, *Macromolecules,* **19**, 2397.
[57] NAVARD, P., 1986, *J. Polym. Sci., Phys. Ed.,* **24**, 435.
[58] MOLDENAERS, P., and MEWIS, J., *Abstract, World Congress III of Chemical Engineering*, p. IV–546.
[59] SUZUKI, M., 1986, M.S. Thesis, Kyoto University.